J Biol Inorg Chem (2015) 20:49–59
DOI 10.1007/s00775-014-1208-4

ORIGINAL PAPER

Reactivity of hexanuclear ruthenium metallaprisms towards nucleotides and a DNA decamer

Lydia E. H. Paul · Bruno Therrien · Julien Furrer

Received: 26 August 2014 / Accepted: 12 October 2014 / Published online: 8 November 2014

Abstract The reactivity of three hexacationic arene ruthenium metallaprisms towards isolated nucleotides and a short DNA strand was investigated using NMR spectroscopy, ESI mass spectrometry, UV/Vis and circular dichroism spectroscopy. The metallaprism built from oxalato-bridging ligands reacts rapidly in the presence of deoxyguanosine monophosphate (dGMP) and deoxyadenosine monophosphate, while the benzoquinonato derivative only reacts with dGMP. On the other hand, the larger metallaprism incorporating naphtoquinonato bridges remains stable in the presence of nucleotides. The reactivity of the three hexacationic metallaprisms with the decameric oligonucleotide $d(CGCGATCGCG)_2$ was also investigated. Analysis of the NMR, MS, UV/Vis and CD data suggests that no adducts are formed between the oligonucleotide and the metallaprisms, but electrostatic interactions, leading to partial unwinding of the double-stranded oligonucleotide, were evidenced.

Keywords Ruthenium · Metallaprisms · Nucleotides · DNA interaction

Electronic supplementary material The online version of this article (doi:10.1007/s00775-014-1208-4) contains supplementary material, which is available to authorized users.

L. E. H. Paul · J. Furrer (✉)
Departement für Chemie und Biochemie, Universität Bern, 3012 Bern, Switzerland
e-mail: julien.furrer@dcb.unibe.ch

B. Therrien
Institut de Chimie, Université de Neuchâtel, 2000 Neuchâtel, Switzerland

Abbreviations

AA	Amino acid
dhbq	2,5-Dihydroxy-1,4-benzoquinonato
dhnq	5,8-Dihydroxy-1,4-naphthoquinonato
DOSY	Diffusion-ordered spectroscopy
ESI	Electrospray ionization
oxa	Oxalato
tpt	2,4,6-Tri(pyridin-4-yl)-1,3,5-triazine

Introduction

Ruthenium complexes are known to be active against cancer cells for more than 60 years [1, 2]. However, their promising biomedical properties were forgotten for some time [3–5], and only 30 years later the research was reactivated by Clarke et al. [2]. While maintaining a high cytotoxicity, most ruthenium-based complexes show lesser side effects when compared to platinum-based drugs [6]. Another benefit of using ruthenium instead of platinum is that two oxidation states (+2 and +3) show activity against cancerous tissues.

The most prominent examples for drug candidates containing ruthenium in oxidation state +3 are NAMI-A [7], developed by the group of Sava, and NKP1339, designed by Keppler et al. [8]. Despite structural similarities, both complexes possess very different modes of action and targets. Multiple interactions with various biomolecules have been identified for NAMI-A, while NKP1339 is most likely binding to DNA [9]. Both complexes are already in or short before entering phase II clinical trials [7, 9, 10].

RAPTA-T and RM175 have been developed in the groups of Dyson and Sadler, respectively, and possess a ruthenium center in the oxidation state +2. Extensive studies were carried out to determine their biological targets and

very recent results show that RAPTA-T attacks histones among other biomolecules [11], while for RM175, DNA, and in particular guanine residue, was identified as the primary target [9].

Exploiting the biological potential of arene ruthenium complexes, our group follows a different approach, which combines the advantages of arene ruthenium complexes and cage-like shaped molecules for cancer treatment [12–14]. These relatively large cage compounds can be advantageous for drug delivery into cancer cells due to the enhanced permeability and retention (EPR) effect, as previously described by Maeda et al. [15, 16]. Due to the increased permeability of cancer tissue compared to healthy tissue, a higher uptake of larger molecules into tumors is observed. For this reason, the large molecules themselves can be used either as drugs or employed as carriers for smaller drug molecules to be delivered directly to their cellular target; the small molecules being entrapped in the cavity of the cage [17].

Nuclear magnetic resonance (NMR) spectroscopy is a useful and versatile technique for investigating the biological activity of metal-based compounds, as well as the reactivity and behavior of selected ruthenium complexes towards biomolecules [18–23]. With the help of this method, it is possible to assess the structure of the reaction products and/or quantify the reaction itself. The application of different NMR experiments showed that the tested hexanuclear ruthenium metallaprisms form degradation products in the presence of certain amino acids [21–23]. The fastest reactions were observed with the smallest metallaprisms $[\mathbf{1}]^{6+}$ ($[(p\text{-cymene})_6Ru_6(tpt)_2(oxa)_3]^{6+}$), followed by $[\mathbf{2}]^{6+}$ ($[(p\text{-cymene})_6Ru_6(tpt)_2(dhbq)_3]^{6+}$) and finally by the largest metallaprism $[\mathbf{3}]^{6+}$ ($[(p\text{-cymene})_6Ru_6(tpt)_2(dhnq)_3]^{6+}$), for which the kinetic of formation was slow. In some cases, a dismantling of the metallaprisms with the loss of tpt and the linkers was observed and coordination of the basic amino acids Arg, His and Lys occurred. Experimental data suggested the formation of chelates. The kinetics of reactions with amino acids strongly varies, depending on the size and strength of the organic linkers. Interestingly, metallaprism $[\mathbf{1}]^{6+}$ was also the most reactive, since formation of at least one degradation product was observed with all tested amino acids, while metallaprism $[\mathbf{3}]^{6+}$ was the most stable, since formation of degradation products was only observed with Arg, His, and Lys. In all investigated cases, the formation of degradation products of the general formula $[(p\text{-cymene})Ru(AA)]^{+}$ was observed.

In 1985, Fichtinger-Schepman et al. [24] showed that cisplatin exhibits its cytotoxicity almost exclusively via binding the G residues of cellular DNA. More recent results show that about 20 % of cisplatin also bind to A and G residues to form crosslinks [25], but currently it is believed that most of the administered cisplatin favors binding to proteins over DNA [26]. Additionally, over 60 % of the platinum is bound to higher molecular mass nucleophiles instead of forming mononuclear adducts with thiol-containing nucleophiles [27, 28]. Since DNA has been considered as the primary target for most platinum-based drugs [29], it also deems necessary to assess the reactivity of the ruthenium metallaprisms towards both isolated nucleotides and a DNA strand. Such studies have been performed for NAMI-A [30, 31], NKP1339 [32] and RM175 [9, 33]. These studies have shown that all three ruthenium complexes interact with DNA, but to different extents: NAMI-A and NKP1339 were shown to bind to A and G residues, but the interactions are far weaker and the structural changes on the DNA less pronounced compared to cisplatin. Similar to cisplatin, RM175 forms mono-functional adducts in solution with G residues via coordination to the N7 atom, while non-covalent interactions are also found, especially arene intercalation and minor groove binding. Therefore, we herein report the investigation of the reaction of three hexacationic arene ruthenium metallaprisms ($[\mathbf{1}](CF_3SO_3)_6$–$[\mathbf{3}](CF_3SO_3)_6$) towards the nucleotides dAMP, dGMP, dCMP and dTMP as well as towards the 10mer DNA strand $d(CGCGATCGCG)_2$. Further characterizations and analyses of the reactions and resulting products have been performed by various methods, including MS, circular dichroism and UV/Vis.

Materials and methods

Chemicals

Chemicals obtained from commercial suppliers were of analytical grade and used as received. The nucleotides dAMP, dCMP, dGMP and dTMP were obtained from Sigma Aldrich and the oligonucleotide $d(CGCGATCGCG)_2$ was ordered from Microsynth AG. The decamer was chosen because its NMR spectrum has been completely assigned [34, 35], and it forms a complete turn including a minor and a major groove in the double helix [36]. The ruthenium metallaprisms $[\mathbf{1}](CF_3SO_3)_6$, $[\mathbf{2}](CF_3SO_3)_6$ and $[\mathbf{3}](CF_3SO_3)_6$ were synthesized according to published methods [12, 13, 37].

NMR spectroscopy

If not otherwise stated, all experiments were carried out by mixing the metallaprisms $[\mathbf{1}](CF_3SO_3)_6$–$[\mathbf{3}](CF_3SO_3)_6$ in 0.5 mL D_2O with six equivalents of the nucleotides. For the experiments with the decameric oligonucleotide, a stock solution of $d(CGCGATCGCG)_2$ in D_2O (containing 0.01 % NaN_3 and 10 mM Na_2HPO_4/KH_2PO_4; $c = 3.575$ mM) was

prepared. Afterwards, solutions of the oligonucleotide were incubated with the compounds at a 1:1 molar ratio.

All reactions were first monitored by 1D ^{1}H NMR spectroscopy. All experiments were undertaken at pD = 7, i.e., close to the pH value of the bloodstream. The pD values of D_2O solutions were measured using a glass electrode and addition of 0.4 to the pH meter reading [38, 39]. To mimic physiological conditions as closely as possible during the experiments, oxygen was not excluded from solutions.

Nuclear magnetic resonance data were acquired at a temperature of 37 °C using a Bruker AvanceII 500 MHz NMR spectrometer, equipped with an inverse 1.7 mm triple channel (^{1}H, ^{31}P, ^{13}C) *z*-gradient microprobe head. All 1D ^{1}H NMR data were measured with 16–64 transients into 32k data points over a width of 15 ppm using a classical presaturation to eliminate the water resonance. A relaxation delay of 6 s was applied between transients.

2D ^{1}H–^{1}H NMR COSY data were acquired over a frequency width of 12 ppm in both F_2 and F_1 into 2k complex data points in F_2 (acquisition time = 213 or 170 ms) using 128 or 256 t_1 increments. A relaxation delay of 2 s between transients was used for all experiments. The data were recorded using 4 or 8 transients, depending on the samples. The water resonance was suppressed by means of a presaturation routine.

2D ^{1}H-DOSY NMR experiments were acquired with a standard pulsed-gradient stimulated echo (LED-PFGSTE) sequence containing bipolar gradients [40, 41]. For each data set, 4k complex points were collected. A 2-s recycle delay was used between scans for data shown. The number of scans ranged from 16 to 64, and it was adapted to each sample. All NMR data were processed using Topspin (Version 3.0, Bruker Switzerland) and Dynamics Center (Version 2.2, Bruker BioSpin Switzerland).

Mass spectrometry studies

Electrospray ionization mass spectrometry (ESI MS) analyses were performed on a LTQ Orbitrap XL mass spectrometer (Thermo Fisher Scientific, Bremen, Germany), equipped with a nanoelectrospray ion source.

The three metallaprisms, using each time 1 mg of the corresponding triflate salts (([**1**](CF$_3$SO$_3$)$_6$–[**3**](CF$_3$SO$_3$)$_6$)) in 1 mL H_2O, were incubated with the selected nucleotide at a 1:6 molar ratio for 48 h at 37 °C. Similarly, for analyzing the DNA samples, the three compounds were dissolved in a stock solution of the oligonucleotide in H_2O to reach a 1:1 molar ratio, and incubated for 48 h at 37 °C. Then, all samples were analyzed in the positive ion mode with a voltage of +700 V applied to the glass emitter (New Objective, Woburn, MA, USA). The tube lens was at +150 V and the transfer capillary was held at 200 °C. Spectra were acquired in the FTMS mode over a range of *m*/*z* 100–2,000 with a resolution of 100,000 at *m*/*z* 400. Calibration of the instrument was performed with ProteoMass LTQ/FTHybrid ESI positive mode calibration mix (Supelco Analytical, Bellefonte, PA, USA). The Xcalibur software package (Xcalibur 2.0.7, Thermo Fisher Scientific) was used for instrument control and data processing.

Circular dichroism studies

The circular dichroism (CD) spectra of the oligonucleotide in the presence or absence of the metallaprisms were accumulated on a J-715 Jasco Spectropolarimeter (with Xe lamp, purged with nitrogen) over a wavelength range of 700–200 nm using a Hellma Suprasil R 100-QS 0.1 cm cuvette quartz cuvette and corrected for buffer signal contribution measured under identical conditions. The metallaprisms [**1**](CF$_3$SO$_3$)$_6$–[**3**](CF$_3$SO$_3$)$_6$ were dissolved in the DNA stock solution in buffered H_2O (10 mM PBS + 0.01 % NaN_3) and incubated for 0, 24 and 48 h before data collection. For each sample, the mixture was scanned three times using a rate of 50 nm/min at 20 °C.

UV/Vis studies

All UV/Vis spectra were recorded on a Cary 100 Bio UV–Visible spectrometer over a wavelength range of 800–190 nm using 1.0 cm quartz cells. The spectra were corrected for buffer signal contribution and measured under identical conditions. For the measurements, a stock solution of the DNA sample (c = 10 μM) was first prepared in buffered solution and UV/Vis spectra were recorded directly after folding of the double strand. The measurement was repeated after 24 h to ensure stability in solution. Afterwards, each metallaprism was dissolved in this stock solution to achieve a 1:1 molar ratio. The solution was mixed properly and spectra were recorded directly thereafter and again after a 24 h incubation period.

For the titration experiment, another stock solution of the DNA sample was prepared (c = 10 μM) as well as a solution of [**3**](CF$_3$SO$_3$)$_2$ in buffer (c = 100 μM). The solution of [**3**](CF$_3$SO$_3$)$_2$ was then added stepwise to the DNA solution and UV/Vis spectra were recorded subsequently after a 5-min incubation period. As negative control, the experiment was repeated using pure buffer solution.

Results and discussion

Reactions with nucleotides

First, we assessed the general reactivity of the metallaprisms [**1**](CF$_3$SO$_3$)$_6$–[**3**](CF$_3$SO$_3$)$_6$ towards isolated nucleotides (dAMP, dCMP, dGMP, dTMP) in D_2O by

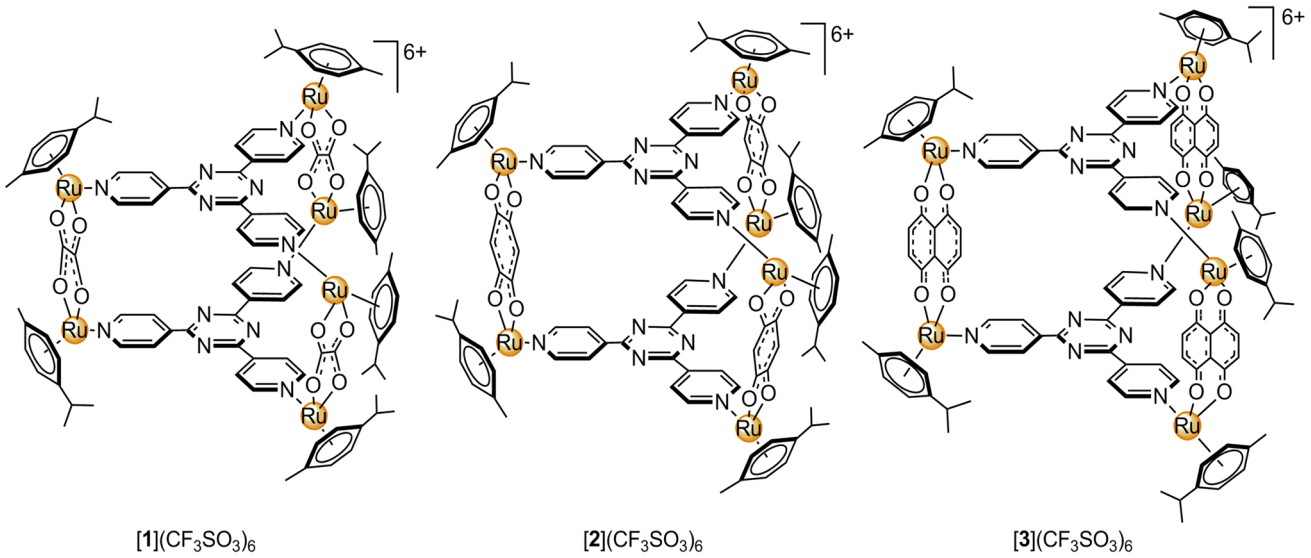

Fig. 1 Structure of the hexacationic metallaprisms $[\mathbf{1}]^{6+}$, $[\mathbf{2}]^{6+}$ and $[\mathbf{3}]^{6+}$

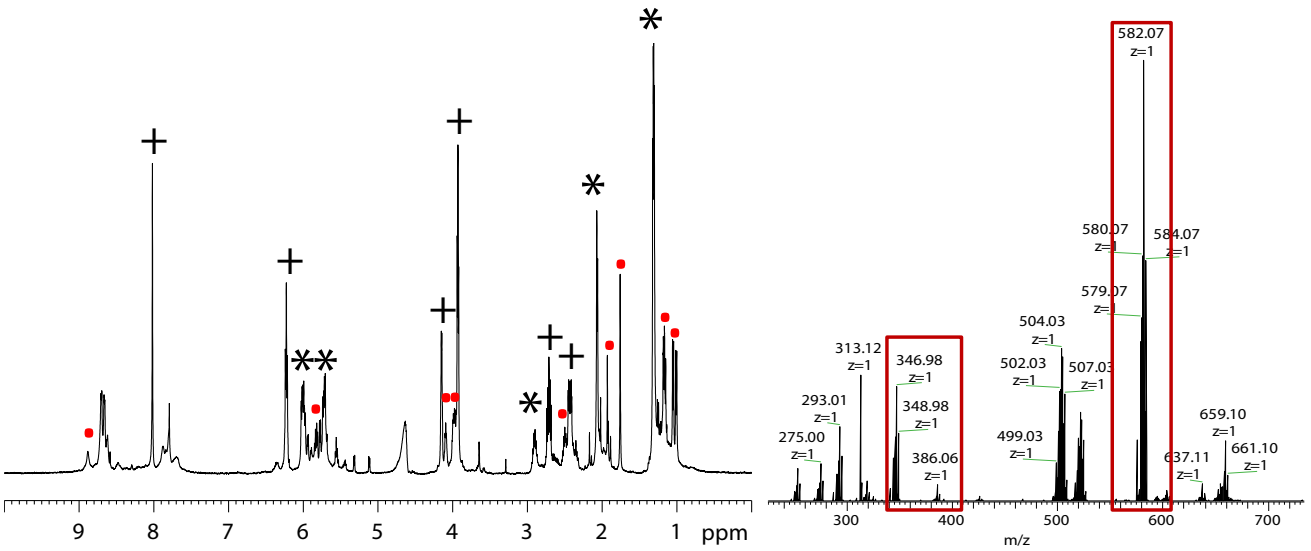

Fig. 2 ^{1}H NMR spectrum of the mixture $[\mathbf{1}]^{6+}$:dGMP (molecular ratio 1:6) recorded after $t = 24$ h (*left side*) and the corresponding ESI mass spectrum (*right side*). In the NMR spectrum, resonances for the *p*-cymene protons of $[\mathbf{1}]^{6+}$ are indicated by (*Asterisks*), resonances for free dGMP by (+) and resonances of the new species by (*Dots*). In the ESI mass spectrum, the peaks corresponding to free dGMP and the degradation product $[(p\text{-cymene})\text{Ru(dGMP)}]^{+}$ are framed (*m/z* 348.98 and 582.07, respectively)

NMR spectroscopy. Reference ^{1}H NMR spectra of the metallaprisms and of the nucleotides are given in Fig. S1 and S2, and the molecular structures of the hexanuclear arene ruthenium complexes are presented in Fig. 1.

Reaction of $[\mathbf{1}]^{6+}$ with nucleotides

Deoxyguanosine monophosphate (dGMP) is an established target for metal-based drugs, in particular for cisplatin and oxaliplatin, but also for NKP1339 and RM175 [9, 32]. The ^{1}H spectrum recorded directly after mixing and dissolving [**1**]$(CF_3SO_3)_6$ and dGMP in D_2O exhibited additional resonances besides the resonances of free dGMP and of the metallaprism (Fig. 2). Notably, the proton H8 of dGMP experienced a typical low-field shift attributable to the coordination of the ruthenium via the N7 atom of dGMP (Fig. 2), as described for other organometallic compounds [42]. Other minor peaks were visible in the regions of tpt and *p*-cymene, but characterization was not attempted due to the very low concentration of the new products. After

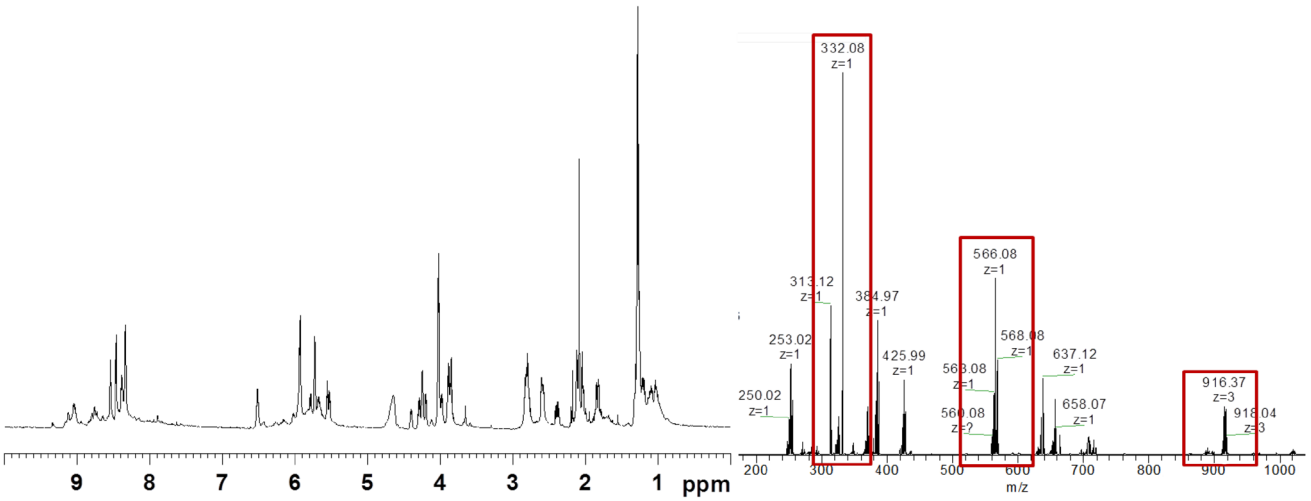

Fig. 3 ^{1}H NMR spectrum of the mixture $[\mathbf{1}]^{6+}$:dAMP (molecular ratio 1:6) recorded at $t = 24$ h (*left side*) and the corresponding mass spectrum (*right side*). In the mass spectrum, the peaks corresponding to free dAMP, the degradation product [(*p*-cymene)Ru(dAMP)]$^{+}$ and the free assembly $[\mathbf{1}]^{6+}$ are framed with *red boxes* (*m/z* 332.08; 566.08 and 916.37, respectively)

24 h reaction time, the reaction reaches equilibrium, but remains incomplete. A 2D DOSY spectrum confirmed that a new species was present in solution together with the intact metallaprism and dGMP (Fig. S3). The exact nature of the new species was determined with the help of ESI mass spectrometry (Fig. 2): the peak at *m/z* 582.07 being assigned to a mononuclear degradation product corresponding to [(*p*-cymene)Ru(dGMP)]$^{+}$.

The ^{1}H spectrum recorded after 24 h for the mixture $[\mathbf{1}]^{6+}$:dAMP showed many additional resonances adjacent to the resonances of free dAMP and the metallaprism $[\mathbf{1}]^{6+}$. Similar to dGMP, the new resonances suggest a coordination of dAMP to the Ru atom and formation of new adducts. As for dGMP, ^{1}H NMR spectra indicate that the reaction reaches equilibrium after 24 h reaction time, but remains incomplete. Besides new peaks belonging to a main adduct, other minor peaks were visible, especially additional H2 and H8 resonances of dAMP and additional *p*-cymene resonances. Characterization was also not attempted due to the very low concentration of these minor products. Formation of the [(*p*-cymene)Ru(dAMP)]$^{+}$ adduct was confirmed with the help of ESI mass spectrometry. Aside from peaks at *m/z* 916.37 corresponding to $\{[(p\text{-cymene})_6Ru_6(oxa)_3(tpt)_2](CF_3SO_3)_3\}^{3+}$ and 332.08 for dAMP, a peak was found at *m/z* 568.08 which is consistent with the newly formed complex [(*p*-cymene)Ru(dAMP)]$^{+}$. Both the NMR and MS data confirmed that the reaction between dAMP and $[\mathbf{1}]^{6+}$ was not complete, since unreacted nucleotide and intact $[\mathbf{1}]^{6+}$ were also detected in solution (Fig. 3). Similar to dGMP, only one kind of degradation product could be identified in the mass spectrum.

The reactions between $[\mathbf{1}]^{6+}$ and dCMP or dTMP showed the appearance of new very weak resonances in the ^{1}H spectrum after 24 h reaction time. Brief analyses (Fig. S4A and B) revealed that these resonances do not belong to the [(*p*-cymene)Ru(dCMP)]$^{+}$ and [(*p*-cymene)Ru(dTMP)]$^{+}$ adducts, but rather that water may interact/bind on the assembly, as already observed for the metallaprism alone [23]. Accordingly, no peaks corresponding to the hypothetical complexes [(*p*-cymene)Ru(dCMP)]$^{+}$ and [(*p*-cymene)Ru(dTMP)]$^{+}$ were visible in the respective ESI mass spectra. The inertness of metallaprism $[\mathbf{1}]^{6+}$ towards dCMP and dTMP is in contrast with other complexes such as $[(\eta^6\text{-bip})Ru(en)Cl]^{+}$ and Ru–, Rh– and Os–pta complexes. For $[(\eta^6\text{-bip})Ru(en)Cl]^{+}$ a 5′-phosphate adduct and a minor N3 adduct with 5′-CMP, as well as a phosphate adduct and a N3 adduct with 5′-TMP were evidenced [43]. For the Ru–, Rh– and Os–pta complexes the N7 position on guanine was the preferred donor atom for coordination to the metal complexes [44], but the pyrimidine nucleosides were also observed to bind to ruthenium complexes, although their affinity was low. The fragmentation pattern in the ESI–MS spectra was characterized by the loss of pta, and suggested a η^2-N6∩N7 coordination mode [44].

Reaction of $[\mathbf{2}]^{6+}$ with nucleotides

In the ^{1}H NMR spectrum of the mixture $[\mathbf{2}]^{6+}$:dGMP recorded directly after mixing the components in D_2O, additional weak resonances adjacent to the resonances of the *p*-cymene residue of the metallaprism appeared. Overall, all resonances are significantly broadened, which can indicate an ongoing reaction. The ^{1}H spectrum recorded after 24 h (Fig. S5A) shows that additional resonances appeared in the spectrum, and that the resonance's intensity

of dGMP and $[\mathbf{2}]^{6+}$ decreased considerably. Equilibrium seems to be reached after 10 h, since the ^{1}H NMR spectrum matches the one recorded after 24 h (Fig. S5A). Besides new peaks belonging to a main adduct, other minor peaks are visible, especially in the regions of H8 and *p*-cymene, but characterization was also not attempted due to the very low concentration of these products. Noteworthy, after 24 h, the resonance for the H8 purine proton was significantly shifted downfield ($\delta = 8.78$ ppm, Fig. S5A & S5B). Similar low-field shifts were observed previously by Sheldrick et al. upon coordination of N7 of dGMP to a metal center [42, 45]. The 2D DOSY NMR spectrum of this mixture of $[\mathbf{2}]^{6+}$ and dGMP shows three distinct diffusion coefficients corresponding to three different molecular species present in the solution (Fig. S5B). Two diffusion coefficients fit with the intact metallaprism $[\mathbf{2}]^{6+}$ and the free nucleotide dGMP; the third diffusion coefficient corresponds to the degradation product $[(p\text{-cymene})\text{Ru(dGMP)}]^{+}$.

The $[(p\text{-cymene})\text{Ru(dGMP)}]^{+}$ adduct was confirmed with the help of ESI mass spectrometry. As with $[\mathbf{1}]^{6+}$, we found a peak at *m*/*z* 582.07, which belongs to the degradation product $[(p\text{-cymene})\text{Ru(dGMP)}]^{+}$. Intriguingly, neither the peaks from the intact metallaprism nor peaks characteristic for other degradation products were found in the spectrum. Some peaks belonging to unidentified fragments of the metallaprism were, however, visible (Fig. S6).

The reactions between $[\mathbf{2}]^{6+}$ and dAMP, dCMP and dTMP were investigated using the same methodology. Although additional resonances and broadened resonances appeared in the NMR spectra, no interactions between the metallaprism and the three nucleotides were identified (Fig. S7 and S8). As an example, the ESI mass spectrum of dAMP and $[\mathbf{2}]^{6+}$ only shows peaks that can be assigned to either the free nucleotide (*m*/*z* 332.08) or the intact metallaprism (*m*/*z* 966.05; 687.55) (Fig. S9). These results followed the tendency we previously observed with amino acids, where $[\mathbf{2}]^{6+}$ was less reactive than $[\mathbf{1}]^{6+}$ [21–23].

Reaction of $[\mathbf{3}]^{6+}$ with nucleotides

The spectra monitoring the reaction of $[\mathbf{3}]^{6+}$ with the nucleotides showed that $[\mathbf{3}]^{6+}$ remains inert in all cases (Fig. S10 and S11). All ^{1}H NMR spectra only exhibited the resonances of the individual components. A peak for the intact metallaprism was found at *m*/*z* 1,016.07 in the spectrum with dGMP meaning the assembly remains stable under these conditions. As an example, Fig. 4 shows the ^{1}H NMR spectrum of the reaction between $[\mathbf{3}]^{6+}$ and dGMP in comparison with the spectra for the isolated components as well as the DOSY spectrum of the mixture. A comparison of all spectra shows that the ^{1}H NMR spectrum of the mixture $[\mathbf{3}]^{6+}$:dGMP (Fig. 4 spectrum C) can be superimposed with the ^{1}H NMR spectra of free $[\mathbf{3}]^{6+}$ and

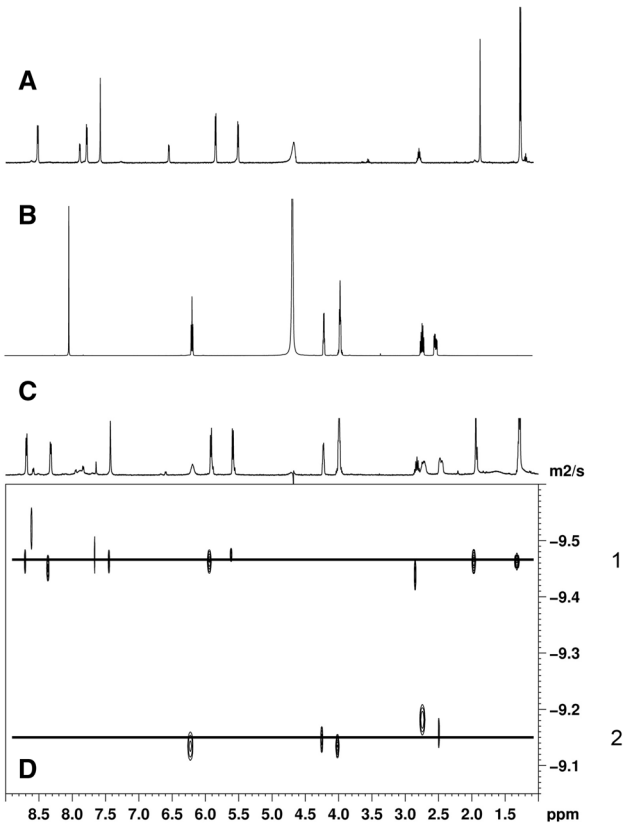

Fig. 4 ^{1}H NMR spectrum of $[\mathbf{3}]^{6+}$ in D_2O (**a**), ^{1}H NMR spectrum of dGMP (**b**), ^{1}H NMR spectrum of the mixture of $[\mathbf{3}]^{6+}$:dGMP (molar ratio 1:6) (**c**), DOSY NMR spectrum of the mixture of $[\mathbf{3}]^{6+}$:dGMP (molar ratio 1:6) (**d**). In the DOSY spectrum, line 1 represents the free metallaprism, line 2 free dGMP

dGMP (Fig. 4 spectrum B and 4 spectrum A, respectively). Similarly, the DOSY spectrum of the mixture $[\mathbf{3}]^{6+}$:dGMP (Fig. 4, spectrum D) exhibits only two distinct diffusion coefficients assigned to free $[\mathbf{3}]^{6+}$ and free dGMP. Accordingly, the respective ESI mass spectra showed no evidence of new derivatives (Fig. S12). Therefore, unlike $[\mathbf{1}]^{6+}$ and $[\mathbf{2}]^{6+}$, metallaprism $[\mathbf{3}]^{6+}$ remains inert upon the addition of dGMP.

Following the trend observed with amino acids, metallaprism $[\mathbf{1}]^{6+}$ exhibits the highest reactivity against free nucleotides. In contrast to our previous results with amino acids, a reaction was only observed with the most reactive purine nucleotides dGMP and dAMP and not with the pyrimidine nucleotides dCMP and dTMP. For $[\mathbf{2}]^{6+}$, a reaction is observed only in the presence of dGMP. Finally, $[\mathbf{3}]^{6+}$ did not react with any of the tested nucleotides. The NMR data suggest that coordination of the nucleotide to the Ru fragment takes place via the N7 atom of dGMP and dAMP as also described by Sheldrick et al. [42, 45].

Although the three investigated metallaprisms possess similar structures, their reactivity appears to be quite

different, in agreement with a recent study showing the dynamic ligand exchange process within bipyridyl-linked arene ruthenium metalla-cycles [46]. Indeed, as observed with the metallaprisms, the most stable metalla-cycles was the $[(p\text{-cymene})_4Ru_4(bpy)_2(dhnq)_2]^{4+}$ (bpy = 4,4′-bipyridine), followed by $[(p\text{-cymene})_4Ru_4(bpy)_2(dhbq)_2]^{4+}$ and finally by the oxalato derivative $[(p\text{-cymene})_4Ru_4(bpy)_2(oxa)_2]^{4+}$.

Reaction of the metallaprisms with the decameric oligonucleotide $d(CGCGATCGCG)_2$

NMR and MS studies

After assessing the reactivity of the metallaprisms towards isolated nucleotides, we investigated their potential affinity for a DNA decamer. The metallaprisms possess aromatic groups that could potentially interact (hydrogen bonds and π–π interactions) and intercalate into the minor/major groove of the decamer. Moreover, the hexacationic charge of the metallaprisms can generate electrostatic interactions.

The potential interaction between $d(CGCGATCGCG)_2$ and $[\mathbf{1}]^{6+}$ was first monitored by ^{1}H NMR spectroscopy. Spectra were recorded every 24 h over a period of 4 days. Within this time, the spectra showed no significant changes. Figure 5 shows a comparison of the ^{1}H NMR spectra of the decamer (bottom) and of the mixture decamer:$[\mathbf{1}]^{6+}$ recorded at $t = 0$ h (middle) and $t = 96$ h (top). Over time, the resonances appeared less broadened but no additional resonances were observed that could suggest an ongoing reaction. In general, the resonances of the metallaprisms and of the oligonucleotide were strongly overlapped, which hampered a clear analysis.

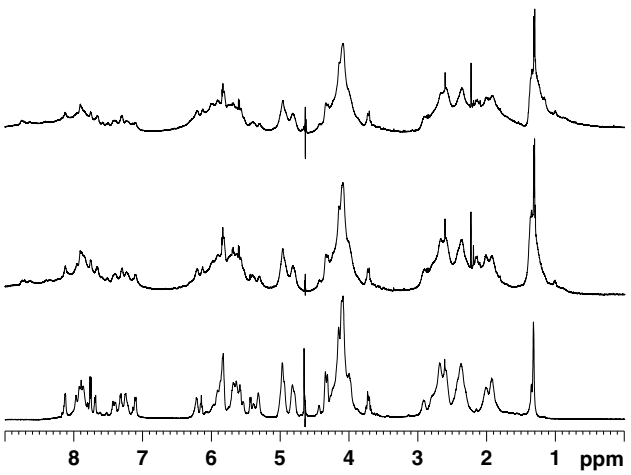

Fig. 5 ^{1}H NMR spectra of the decamer in buffered solution (*bottom*), a 1:1 mixture of the decamer and $[\mathbf{1}]^{6+}$ at $t = 0$ h (*middle*) and at $t = 96$ h (*top*). No significant changes are observed over time, aside from line broadening

The ESI mass spectrum recorded in the negative mode supports the results obtained from the NMR data. In the spectrum, no peaks indicating an adduct formation between the DNA decamer and the metallaprism or a fragment thereof were found (Fig. S13). Also, ESI mass spectrum recorded in the positive mode shows no fragments consistent with adduct formation between the metallaprism and the oligonucleotide (Fig. S14).

The reactions between $[\mathbf{2}]^{6+}$, $[\mathbf{3}]^{6+}$ and $d(CGCGATCGCG)_2$ were also investigated using the same strategy and identical experimental conditions. After 96 h, apart from an overall slight line broadening, no new resonances and no resonances' shifts were observed in the spectrum of the mixture $[\mathbf{2}]^{6+}$:$d(CGCGATCGCG)_2$ (Fig. S17). Attempts to obtain exploitable ESI mass spectra in the negative mode remained unsuccessful, mostly because it was impossible to create a suitable spray to measure the spectrum. However, the ESI mass spectrum recorded in the positive mode shows no fragments that indicate binding of the metallaprism to the decameric oligonucleotide (Fig. S15). The same behavior was observed for the mixture $[\mathbf{3}]^{6+}$:$d(CGCGATCGCG)_2$ recorded after 96 h: The data suggest that no reaction took place (Fig. S18). Both ESI mass spectra of the mixture $[\mathbf{3}]^{6+}$:$d(CGCGATCGCG)_2$ recorded in the positive mode (Fig. S16) and negative mode (Fig. S19) show only peaks characteristic of the oligomer, for instance at *m/z* 791.35 and 907.83 (Fig S16), that are also visible in the reference ESI mass spectrum of the oligonucleotide (Fig. S20).

While the NMR and ESI mass data strongly indicate that the three metallaprisms do not bind to the DNA decamer $d(CGCGATCGCG)_2$, the general line broadening observed in the ^{1}H-NMR spectra of the mixtures could indicate interactions between the metallaprisms and the DNA. The observed line broadening could also be triggered by the insertion of the metallaprisms in the minor/major groove of the DNA. Therefore, to confirm or refute this hypothesis, circular dichroism and UV–Vis measurements were performed.

Circular dichroism

Circular dichroism (CD) spectroscopy is a very useful tool to monitor structural changes in DNA strands. It allows for directly following conformational changes of DNA induced by various molecules. For example, in the presence of metal complexes that bind to DNA, complete inversion, band shift, change of intensity or other changes of the CD bands can be observed in the spectra [47–49]. The CD measurements were carried out under similar conditions as the NMR measurements: The samples were dissolved in buffered solution and incubated at 37 °C for 48 h in total, to ensure equilibrium and to facilitate possible reactions to occur.

Figure 6 shows the CD spectra obtained from the three mixtures metallaprism:DNA (ratio 1:1). The spectrum of the

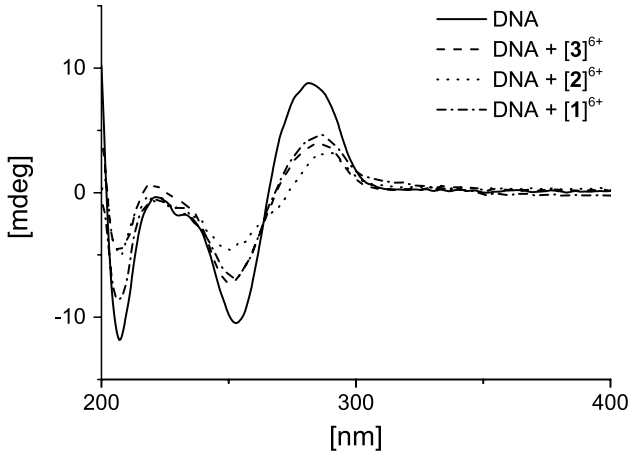

Fig. 6 CD spectra of the DNA oligomer alone in buffered solution as well as in 1:1 mixtures with the metallaprism $[\mathbf{1}]^{6+}$–$[\mathbf{3}]^{6+}$ recorded at $t = 48$ h

isolated DNA strand (solid line) is used for comparison with the spectra recorded after adding the metallaprisms to reach a 1:1 ratio. In general, upon addition of the metallaprisms, no band shifts are observed, but a general decrease of the signal intensity for all bands of the DNA spectrum is observed. The change occurred over time, as emphasized in Fig. S21, which compares the CD spectra of the DNA double strand alone and in the presence of $[\mathbf{1}]^{6+}$ recorded at $t = 0$, 24, and 48 h. As previously shown for palladium and platinum complexes [50, 51], the quenching of the signal intensity could indicate that an interaction occurs between the decamer and the metallaprism, while the secondary structure of the DNA strand is retained [50–52]. For the three metallaprisms considered in this work, this statement appears, however, unlikely since the ruthenium binding would almost certainly cause structural changes in the DNA strand and thereby leading to a different CD spectrum. Fu et al. have shown that upon binding of copper complexes to CT-DNA the bands in the CD spectrum suffer a significant red shift accompanied by a decrease in band intensity [52]. Similar observations were described by Shi et al. using a mononuclear ruthenium complex [53]. Therefore, the CD spectra are in agreement with the NMR and MS data and strongly suggest that chemical bonds are not formed between the metallaprisms and the decamer.

Ionic interactions between the positively charged metallaprisms and the negatively charged DNA backbone, leading to a partial unwinding of the decamer appear more plausible to explain the observed intensity decrease in the CD spectra [54]. It was reported that simple electrostatic interactions of smaller molecules cause no effect on the CD bands, whereas intercalation would increase the intensity of both positive and negative bands. Also, if π-stacking would take place, a strong increase of the intensity for the observed bands would occur [55].

The observed loss of intensity for the CD bands seems therefore to correlate with the size of the metallaprism. As shown in Fig. 6, addition of the smallest metallaprism, $[\mathbf{1}]^{6+}$, has moderate effect on the CD spectrum, while larger changes are observed in the presence of the largest metallaprisms $[\mathbf{2}]^{6+}$ and $[\mathbf{3}]^{6+}$. Considering the size of the DNA grooves (about 12 Å for the minor groove and 22 Å for the major groove) [56] and the size of the metallaprisms, these results are not surprising: the largest metallaprisms $[\mathbf{2}]^{6+}$ and $[\mathbf{3}]^{6+}$ can fit better in the DNA grooves (Fig. S22). Based on these CD measurements, we can confirm that a chemical binding of the ruthenium atom to the nucleotides of the decamer appears unlikely.

UV/Vis spectroscopy

To confirm the results deduced from the CD and NMR experiments, additional UV/Vis spectra were recorded. Previous studies showed that, upon intercalation, the DNA bands shift to higher wavelength and suffer hypochromism [57], while electrostatic interactions between the ligands and DNA lead to hyperchromism due to conformational and structural changes to the DNA molecule. The presence of cations that can bind to the phosphate backbone can alter the secondary DNA structure and thereby lead to hyperchromism, [58], and hyperchromism can also be an indicator for partial uncoiling of the double helix, as observed by Shahabadi et al. [59].

The UV/Vis spectrum of the decamer recorded at $t = 0$ h (Fig. 7a) exhibits two prominent bands between 200 and 300 nm which are typical for an intact double strand, while the spectra of the metallaprisms show very weak bands compared to those of the decamer. The spectra of the three mixtures metallaprism:decamer recorded at $t = 0$ h exhibit the same bands between 200 and 300 as found for the decamer alone. Interestingly, the intensity of these bands significantly increased for the mixtures with $[\mathbf{1}]^{6+}$ and $[\mathbf{2}]^{6+}$ while the band's intensity is slightly reduced for the mixture with $[\mathbf{3}]^{6+}$ (Fig. 7a). For the mixtures with metallaprisms $[\mathbf{1}]^{6+}$ and $[\mathbf{2}]^{6+}$, the increased intensity of the resulting bands is most likely a result of electrostatic interactions between the anionic backbone and the positively charged metallaprisms $[\mathbf{1}]^{6+}$ and $[\mathbf{2}]^{6+}$, which results in a partial unwinding of the DNA decamer. It is known that the wavelength of maximum absorbance of single-stranded DNA does not change but the absorbance increases by 40 % compared to double-stranded DNA, mainly due to increased electronic interactions [60, 61]. For the mixture with $[\mathbf{3}]^{6+}$, the intensity of the absorption bands is indeed lower than those of the free decamer, but no hypso- or bathochromic shift of the two maxima is observed.

In Fig. 7b, the UV/Vis spectra of the mixtures and the decamer recorded after 24 h incubation are shown. As

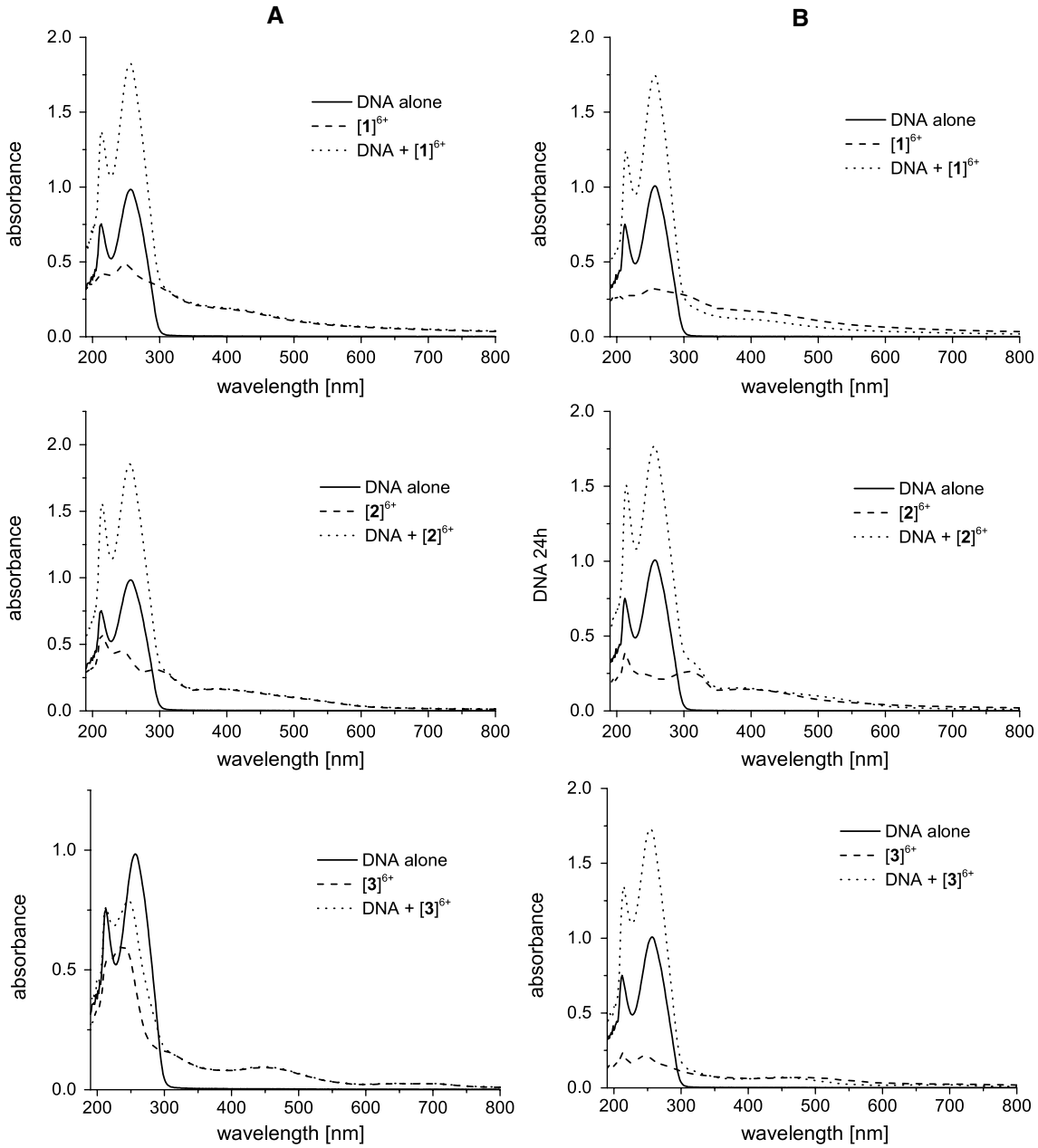

Fig. 7 UV/Vis spectra of the reaction mixtures of the metallaprisms and the decamer. The spectra of the decamer alone were added for comparison. Column **a** shows the spectra recorded at $t = 0$ h (*top* = with $[\mathbf{1}]^{6+}$, *middle* = with $[\mathbf{2}]^{6+}$, *bottom* = with $[\mathbf{3}]^{6+}$), column **b** shows the spectra recorded at $t = 24$ h (*top* = with $[\mathbf{1}]^{6+}$, *middle* = with $[\mathbf{2}]^{6+}$, *bottom* = with $[\mathbf{3}]^{6+}$). The concentrations of the samples are 10 μM for both the decamer and the metallaprism

expected, the spectrum of the decamer remains identical, showing that the DNA is stable in the buffer for at least 24 h. Only after 48 h, partial unwinding of the double strand is observed (Fig. S23). For the mixtures DNA:$[\mathbf{1}]^{6+}$ and DNA:$[\mathbf{2}]^{6+}$, the spectra recorded at $t = 0$ h and $t = 24$ h are identical, while some changes can be noticed in the spectrum of the mixture DNA:$[\mathbf{3}]^{6+}$. For the latter, the intensity of the absorption bands has increased and the spectrum recorded after 24 h is now nearly identical to the spectra of the mixtures DNA:$[\mathbf{1}]^{6+}$ and DNA:$[\mathbf{2}]^{6+}$. This finding suggests that the mixture $[\mathbf{3}]^{6+}$:decamer needs a longer period to reach equilibrium. These differences in the reaction kinetics may be attributed to the different sizes of the metallaprisms: metallaprism $[\mathbf{3}]^{6+}$, being the largest, reaction equilibrium is possibly reached after a longer reaction time.

A closer inspection reveals that the spectra of the free metallaprisms exhibit a general decrease of the intensity

after 24 h, particularly visible for metallaprism $[\mathbf{3}]^{6+}$. Previous NMR studies [21–23] have shown that the metallaprisms $[\mathbf{2}]^{6+}$ and $[\mathbf{3}]^{6+}$ do not disassemble upon the addition of $[Cl^-]$. For $[\mathbf{1}]^{6+}$, NMR spectra suggest that the ruthenium assembly slowly disassembles by losing the tpt moiety and most likely also the oxalato ligand [21]. A similar behavior was observed in the buffer solution used for the optical spectroscopy experiments. ^{1}H- and DOSY NMR spectra (Fig. S24–S27) established that the metallaprisms slowly loss the tpt moiety and/or the linker dhnq/dhbq/oxa. After 24 h, the ^{1}H NMR spectra showed that approximately 9 % of $[\mathbf{3}]^{6+}$ disassembled upon the addition of NaN_3, while approximately 16 % disassembled upon the addition of Na_2HPO_4 (Fig. S24–S25). The loss and the precipitation of the aromatic system therefore explain the observed decrease of the UV/Vis bands.

Conclusions

Apart from cisplatin and platinum drugs derived thereof, ruthenium complexes are probably the most investigated organometallic drug candidates. To evaluate the potential of these drugs and to further improve their performance in anticancer treatments, it is essential to better understand their mode of action and their cellular targets. In this study, the main goal was to assess the reactivity of three hexacationic hexanuclear ruthenium metallaprisms towards nucleotides and a DNA decamer using various NMR, MS, CD and UV/Vis experiments to identify the most likely targets of this type of ruthenium compounds once they have entered cells.

A common feature of the three metallaprisms is their inertness towards the pyrimidine nucleotides dCMP and dTMP, which contrasts with some other arene ruthenium compounds. The reactions with the purine nucleotides dAMP and dGMP showed a distinct reactivity, in line with our previous studies with amino acids [21–23]. In the case of the oxalato derivative $[\mathbf{1}]^{6+}$, reactions were observed with both dAMP and dGMP. For each nucleotide, a degradation product of the general formula [(*p*-cymene)Ru(nucleotide)]$^+$ was identified as the main component in the ESI mass spectrum and in the various NMR spectra. With metallaprism $[\mathbf{2}]^{6+}$, a similar degradation product [(*p*-cymene)Ru(nucleotide)]$^+$ could be identified upon addition of dGMP, but not upon addition of dAMP. Finally, metallaprism $[\mathbf{3}]^{6+}$ was the most unreactive among the three metallaprisms, since no reaction was observed. Interestingly, the reactivity of the three metallaprisms towards nucleotides follows the tendency we have observed towards amino acids, $[\mathbf{1}]^{6+}$ being the most reactive and $[\mathbf{3}]^{6+}$ being the less reactive [21–23].

NMR, MS, CD and UV/Vis experiments with the DNA decamer $d(CGCGATCGCG)_2$ suggest that only electrostatic interactions occur between the negatively charged decameric backbone and the positively charged metallaprisms. However, as shown by CD and UV–Vis, it appears that the electrostatic interactions between the metallaprisms and DNA lead to a partial unwinding of the DNA double strand.

The results presented in this study suggest that DNA appears as a secondary target for the tested hexanuclear ruthenium metallaprisms. On the one hand, only partial unwinding of DNA could be evidenced in the presence of these three metallaprisms; and on the other hand, we have previously shown that the metallaprisms disassemble and form degradation products in the presence of certain amino acids [21–23]. Therefore, in complex biological systems and at therapeutic concentrations (μM), it can be anticipated that a reaction with DNA will be rare, since the metallaprisms will mostly degrade and disassemble in the cytosol. Investigations to determine potential proteins targets and for understanding how these hexacationic metallaprisms are transported into cells are currently undertaken in our laboratories.

Acknowledgments J. F. thanks the Swiss National Science Foundation (Grant No 206021_139078) for financial support. A generous loan of ruthenium chloride hydrate from the Johnson Matthey Technology Center is gratefully acknowledged.

References

1. Dwyer FP, Gyarfas EC, Rogers WP, Koch JH (1952) Nature 170:190–191
2. Clarke MJ (1980) Met Ions Biol Syst 11:231–283
3. Süss-Fink G (2010) Dalton Trans 39:1673–1688
4. Gasser G, Ott I, Metzler-Nolte N (2011) J Med Chem 54:3–25
5. Gianferrara T, Bratsos I, Alessio E (2009) Dalton Trans 38:7588–7598
6. Bergamo A, Sava G (2011) Dalton Trans 40:7817–7823
7. Rademaker-Lakhai JM, van den Bongard D, Pluim D, Beijnen JH, Schellens JHM (2004) Clin Cancer Res 10:3717–3727
8. Trondl R, Heffeter P, Kowol CR, Jakupec MA, Berger W, Keppler BK (2014) Chem Sci 5:2925–2932
9. Bergamo A, Gaiddon C, Schellens JHM, Beijnen JH, Sava G (2012) J Inorg Biochem 106:90–99
10. Groessl M, Hartinger CG, Poleć-Pawlak K, Jarosz M, Dyson PJ, Keppler BK (2008) Chem Biodivers 5:1609–1614
11. Wolters DA, Stefanopoulou M, Dyson PJ, Groessl M (2012) Metallomics 4:1185–1196
12. Barry NPE, Therrien B (2009) Eur J Inorg Chem:4695–4700
13. Govindaswamy P, Linder D, Lacour J, Süss-Fink G, Therrien B (2006) Chem Commun:4691–4693
14. Therrien B (2009) Eur J Inorg Chem:2445–2453
15. Maeda H (2001) Adv Enzyme Regul 41:189–207
16. Matsumura Y, Maeda H (1986) Cancer Res 46:6387–6392
17. Fox ME, Szoka FC, Fréchet JMJ (2009) Acc Chem Res 42:1141–1151
18. Liu H-K, Wang F, Parkinson JA, Bella J, Sadler PJ (2006) Chem Eur J 12:6151–6165

19. Wang F, Xu J, Habtemariam A, Bella J, Sadler PJ (2005) J Am Chem Soc 127:17734–17743
20. Ginzinger W, Mühlgassner G, Arion VB, Jakupec MA, Roller A, Galanski M, Reithofer M, Berger W, Keppler BK (2012) J Med Chem 55:3398–3413
21. Paul LEH, Furrer J, Therrien B (2013) J Organomet Chem 734:45–52
22. Paul LEH, Therrien B, Furrer J (2012) Inorg Chem 51:1057–1067
23. Paul LEH, Therrien B, Furrer J (2012) J Biol Inorg Chem 17:1053–1062
24. Fichtinger-Schepman AMJ, van der Veer JL, den Hartog JHJ, Lohman PHM, Reedijk J (1985) Biochemistry 24:707–713
25. Jamieson ER, Lippard SJ (1999) Chem Rev 99:2467–2498
26. Fuertes MA, Alonso C, Pérez JM (2003) Chem Rev 103:645–662
27. Hermann G, Heffeter P, Falta T, Berger W, Hann S, Koellensperger G (2013) Metallomics 5:636–647
28. Kasherman Y, Sturup S, Gibson D (2009) J Med Chem 52:4319–4328
29. Łęczkowska A, Vilar R (2013) Annu Rep Prog Chem Sect A Inorg Chem 109:299–316
30. Bacac M, Hotze ACG, van der Schilden K, Haasnoot JG, Pacor S, Alessio E, Sava G, Reedijk J (2004) J Inorg Biochem 98:402–412
31. Pluim D, van Waardenburg RCAM, Beijnen JH, Schellens JHM (2004) Cancer Chemother Pharmacol 54:71–78
32. Hartinger CG, Zorbas-Seifried S, Jakupec MA, Kynast B, Zorbas H, Keppler BK (2006) J Inorg Biochem 100:891–904
33. Nováková O, Chen H, Vrána O, Rodger A, Sadler PJ, Brabec V (2003) Biochemistry 42:11544–11554
34. Myari A, Hadjiliadis N, Garoufis A, Malina J, Brabec V (2007) J Biol Inorg Chem 12:279–292
35. Proudfoot EM, Mackay JP, Karuso P (2001) Biochemistry 40:4867–4878
36. Watson JD, Crick FHC (1953) Nature 171:737–738
37. Therrien B, Süss-Fink G, Govindaswamy P, Renfrew AK, Dyson PJ (2008) Angew Chem Int Ed 47:3773–3776
38. Glasoe PK, Long FA (1960) J Phys Chem 64:188–190
39. Mikkelsen K, Nielsen SO (1960) J Phys Chem 64:632–637
40. Morris KF, Johnson CS (1992) J Am Chem Soc 114:3139–3141
41. Morris GA (2002) In: Grant DM, Harris RK (ed) Encyclopedy of nuclear magnetic resonance. Wiley, pp 35–44
42. Korn S, Sheldrick WS (1997) J Chem Soc Dalton Trans:2191–2199
43. Chen H, Parkinson JA, Morris RE, Sadler PJ (2003) J Am Chem Soc 125:173–186
44. Dorcier A, Hartinger CG, Scopelliti R, Fish RH, Keppler BK, Dyson PJ (2008) J Inorg Biochem 102:1066–1076
45. Korn S, Sheldrick WS (1997) Inorg Chim Acta 254:85–91
46. Garci A, Marti S, Schürch S, Therrien B (2014) RSC Adv 4:8597–8604
47. Chang Y-M, Chen CKM, Hou M-H (2012) Int J Mol Sci 13:3394–3413
48. Kypr J, Kejnovská I, Renčiuk D, Vorlícková M (2009) Nucleic Acids Res 37:1713–1725
49. Vorlíčková M, Kejnovská I, Bednářová K, Renčiuk D, Kypr J (2012) Chirality 24:691–698
50. Matesanz AI, Pérez JM, Navarro P, Moreno JM, Colacio E, Souza P (1999) J Inorg Biochem 76:29–37
51. Terenzi A, Ducani C, Blanco V, Zerzankova L, Westendorf AF, Peinador C, Quintela JM, Bednarski PJ, Barone G, Hannon MJ (2012) Chem Eur J 18:10983–10990
52. Fu X-B, Liu D-D, Lin Y, Hu W, Mao Z-W, Le X-Y (2014) Dalton Trans 43:8721–8737
53. Shi S, Geng X, Zhao J, Yao T, Wang C, Yang D, Zheng L, Ji L (2010) Biochimie 92:370–377
54. De Rache A, Kejnovská I, Vorlíčková M, Buess-Herman C (2012) Chem Eur J 18:4392–4400
55. Rajesh J, Rajasekaran M, Rajagopal G, Athappan P (2012) Spectrochim Acta Part A 97:223–230
56. Wing R, Drew H, Takano T, Broka C, Tanaka S, Itakura K, Dickerson RE (1980) Nature 287:755–758
57. Liu J, Zhang T, Lu T, Qu L, Zhou H, Zhang Q, Ji L (2002) J Inorg Biochem 91:269–276
58. Arjmand F, Jamsheera A (2011) Spectrochim Acta Part A 78:45–51
59. Shahabadi N, Kashanian S, Khosravi M, Mahdavi M (2010) Transition Met Chem 35:699–705
60. Thomas R (1954) Biochim Biophys Acta 14:231–240
61. Watson JD, Baker TA, Bell SP, Gann A, Levine M, Losick R (2004) In: Cummings B (ed) Molecular biology of the gene. Pearson Education Inc., pp 125